Available online at www.sciencedirect.com
ScienceDirect
European Journal of Medicinal Chemistry 43 (2008) 1248–1260
EUROPEAN JOURNAL OF MEDICINAL CHEMISTRY
http://www.elsevier.com/locate/ejmech

Original article

Xanthine oxidase-activated prodrugs of thymidine phosphorylase inhibitors

Philip Reigan, Abdul Gbaj, Ian J. Stratford, Richard A. Bryce, Sally Freeman*

School of Pharmacy and Pharmaceutical Sciences, The University of Manchester, Oxford Road, Manchester M13 9PL, UK

Received 26 March 2007; accepted 13 July 2007
Available online 6 August 2007

Abstract

Thymidine phosphorylase (TP) is over-expressed in various tumour types and plays an important role in tumour angiogenesis, growth, invasion and metastasis. The enzymatic activity of TP is required for the angiogenic effect of TP, therefore, inhibitors of TP are of significant interest in cancer chemotherapy. A series of xanthine oxidase (XO) activated prodrugs of known inhibitors of TP have been designed and synthesized with the ultimate intent of improving tumour selectivity and pharmacokinetic characteristics. These prodrugs were not inhibitors of TP, but were selectively oxidized by XO at C-2 and/or C-4 of the uracil ring moiety to generate the desired TP inhibitor. Molecular modelling of both the TP inhibitors and XO-activated prodrugs rationalized their binding in the active site of the human TP crystal structure.

Keywords: Thymidine phosphorylase; Xanthine oxidase; Enzyme inhibition; Prodrug activation

1. Introduction

Thymidine phosphorylase (TP, EC 2.4.2.4) is a highly expressed protein in many solid human tumours, and the level of expression is associated with tumour neovascularization, invasiveness and metastasis [1]. TP is predominantly expressed in hypoxic regions of solid tumours [2], promoting tumour growth by angiogenesis, metastasis and suppressing apoptosis [3,4]. TP is also known as platelet-derived endothelial cell growth factor (PD-ECGF), a novel angiogenic protein, distinct from other angiogenic growth factors, since it exerts its actions through its enzymatic activity, as both site-directed mutagenesis of active-site residues and inhibitors prevent the angiogenic activity of TP [3,4]. TP catalyzes the reversible phosphorolysis of thymidine (**1**) to thymine (**2**) and α-D-2-deoxyribose-1-phosphate (**3**) (Scheme 1). The dephosphorylated product, D-2-deoxyribose (**4**) has been shown to have chemotactic activity *in vitro* and angiogenic activity *in vivo* [3,4] and is considered to play a key role in the invasiveness and metastasis of TP-expressing solid tumours [1].

Since TP is over-expressed in tumours, the protein is an attractive cancer chemotherapy target for selective inhibition of TP-dependent angiogenesis and subsequent inhibition of tumour growth. In addition, specific inhibitors of human TP could also enhance the efficacy of thymidine analogues such as 5-fluoro-2′-deoxyuridine and 5-iodo-2′-deoxyuridine, which would no longer be metabolized and inactivated by TP [5]. The classical TP inhibitors include 6-amino-5-bromouracil (6A5BU, **5**) [6–8] and 7-deazaxanthine (7-DX, **6**) (Fig. 1), which was the first purine derivative to display inhibition of both *E. coli* TP and angiogenesis in a chorioallantoic membrane assay [9]. More potent nanomolar inhibitors of human TP are 5-chloro-6-[(2-iminopyrrolidin-1-yl)methyl]uracil hydrochloride (TPI, **7**) (IC_{50} 35 nM, K_i 20 nM) [10,11] and 5-bromo-6-[(2-aminoimidazol-1-yl)methyl]uracil hydrochloride (**8**) (IC_{50} 20 nM) (Fig. 1) [12], these cationic tight-binding

Abbreviations: TP, thymidine phosphorylase; XOR, xanthine oxidoreductase; XO, xanthine oxidase; XDH, xanthine dehydrogenase; PD-ECGF, platelet-derived endothelial cell growth factor; 6A5BU, 6-amino-5-bromouracil; 7-DX, 7-deazaxanthine; TPI, 5-chloro-6-[(2-iminopyrrolidin-1-yl)methyl]uracil hydrochloride; AO, aldehyde oxidase.

* Corresponding author. Tel.: +44 (0) 161 275 2366; fax: +44 (0) 161 275 2396.
E-mail address: sally.freeman@manchester.ac.uk (S. Freeman).

0223-5234/$ - see front matter © 2007 Elsevier Masson SAS. All rights reserved.
doi:10.1016/j.ejmech.2007.07.015

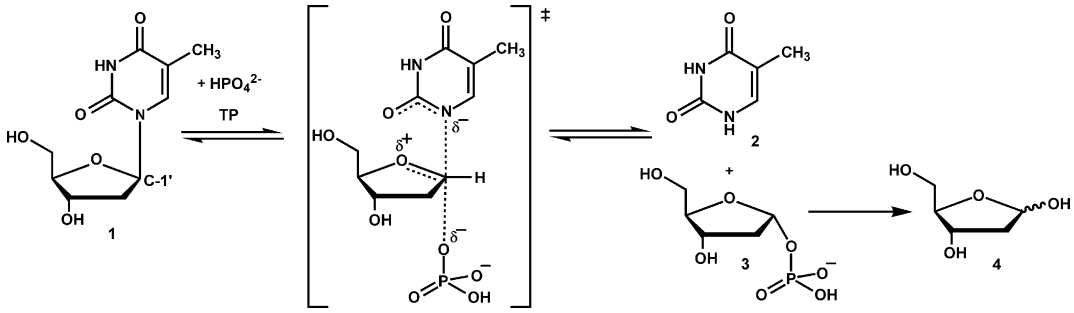

Scheme 1. The catalytic action of TP.

inhibitors have been proposed to mimic the oxocarbenium ion-like transition state for thymidine phosphorolysis (Scheme 1) [13]. However, despite the nanomolar potency of these nucleobase-derived inhibitors, their ionic nature leads to poor pharmacokinetic properties [12].

TP inhibitors are reportedly selective to cells expressing TP and this expression correlates with hypoxia in tumours [2]. However, further selectivity and improved pharmacokinetic characteristics could be achieved using the xanthine oxidase (XO, EC 1.1.3.22) prodrug strategy, since XO activity and expression is increased under hypoxic conditions [14–16]. Furthermore, human tissues have increased XO activities in colorectal and prostate tumours as compared to their corresponding normal tissues [17,18]. In addition, XO levels in human brain tumour tissues have been found to be elevated compared to that of normal brain tissue, in meningioma and astrocytoma oncotypes [19]. The selective inhibition of TP in tumours *via* an enzymatically-activated prodrug approach would be advantageous, since TP is also expressed at high levels in human blood platelets and normal tissues, such as the salivary glands, ovaries and brain, and in addition TP plays an important role in nucleotide homeostasis [5].

XO catalyzes the oxidation of hypoxanthine (**9**) and xanthine (**10**) to uric acid (**11**) (Scheme 2). In addition, XO bioreductively metabolizes a number of quinone-based anticancer drugs [20,21] and a range of nitroimidazoles [12,22]. 2/4-Nitroimidazole prodrugs of the 6-[(2/4-aminoimidazol-1-yl)methyl]uracils, including **8**, which exploit the reductive half-reaction at the FAD-site of XO have been reported previously [12]. The oxidation reaction

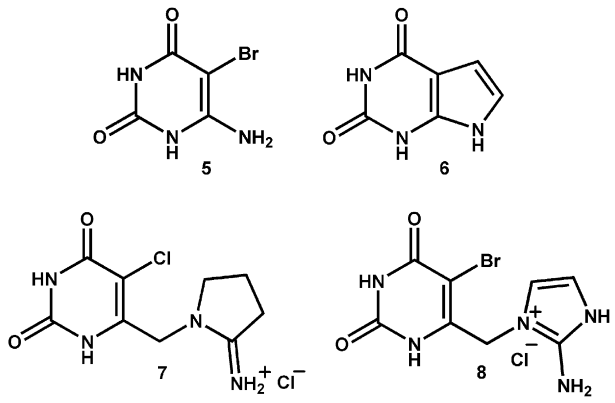

Fig. 1. Uracil-based TP inhibitors.

catalyzed at the molybdenum–pterin site of XO has been previously utilized to increase the bioavailability, solubility and selectivity of 2′-*F*-ara-ddI (2′-*F*-ara-ddP), an anti-HIV nucleoside [23] and acyclovir (6-deoxyacyclovir), an anti-herpetic agent [24], which like TPI are administered orally. The TP inhibitors, being uracil-based heterocycles, are attractive targets for activation by the oxidative reaction catalyzed by XO.

Here, we report the synthesis and evaluation of a series of XO-activated prodrugs of the TP inhibitors 6A5BU (**5**), 7-DX (**6**) and TPI (**7**). The XO prodrugs of the known TP inhibitors were designed to lack carbonyl substitution at C-2 and/or C-4 of the uracil ring system (Scheme 3). The rationale is that these prodrugs would be converted by selective oxidation, at the molybdenum–pterin site of XO, to the active TP inhibitor. The absence of the carbonyl substituent at the C-2 and/or C-4 positions of the prodrugs may increase lipophilicity and bioavailability and therefore improve the pharmacokinetics of the TP inhibitors. We have previously communicated the initial findings of this research [25], here extended to detail the chemical synthesis and enzymology, and include molecular modelling studies using the human TP crystal structure.

2. Results and discussion

2.1. Chemistry

The proposed XO-activated prodrugs of 6A5BU (Scheme 3A): 6-amino-5-bromo-3*H*-pyrimidin-4-one (**12**), 6-amino-5-bromo-1*H*-pyrimidin-2-one (**13**) and 6-amino-5-bromopyrimidine (**14**), were synthesized by electrophilic substitution of the appropriate 6-aminopyrimidine with molecular bromine (Scheme 4). The conditions required optimization to prevent di- or even tri-bromination of the 6-amino-pyrimidines. The bromination of 6-amino-*3H*-pyrimidin-4-one (**21**) and 6-amino-*1H*-pyrimidin-2-one (**22**) was possible at room temperature [26], whereas the bromination of 6-amino-pyrimidine (**23**) required heating at 55–60 °C, to activate the aminopyrimidine ring [27].

The proposed series of XO-activated prodrugs of 7-DX (Scheme 3B): 7*H*-pyrrolo[2,3-*d*]pyrimidin-4(3*H*)-one (**15**), 7*H*-pyrrolo[2,3-*d*]pyrimidin-2(1*H*)-one (**16**) and 7*H*-pyrrolo[2,3-*d*]pyrimidine (**17**), were synthesized *via* cyclo-condensation reactions. The synthesis of **16** was initially attempted by the same method used to obtain 7-DX [28], using **22** and chloroacetaldehyde (Scheme 5A), however, this reaction gave

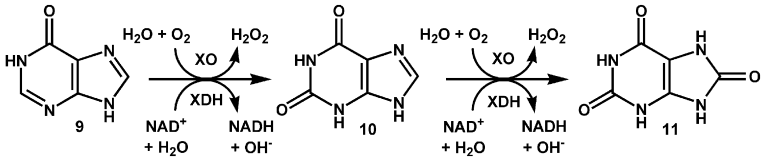

Scheme 2. The catalytic action of XO.

6*H*-imidazo[1,2-*c*]pyrimidin-5-one (**24**) as the major product [29]. Prodrug **15**, was synthesized by cyanoacetic ester synthesis by reaction of bromoacetaldehyde diethyl acetal (**25**) and excess ethyl cyanoacetate (**26**) to yield ethyl 2-cyano-4,4-diethoxybutanoate (**27**). The condensation of **27** with thiourea, gave the desired diacetal protected uracil, 6-amino-5-(2,2-diethoxyethyl)-2-thiouracil (**28**). Acid hydrolysis of **28** gave 2-mercapto-7*H*-pyrrolo[2,3-*d*]-pyrimidin-4(3*H*)-one (**29**) which was then desulphurized by hydrogenolysis with Raney nickel to give **15** (Scheme 5B) [30]. The chlorination of **15** at C-4 with $POCl_3$, followed by palladium catalyzed hydrogenation afforded prodrug **17** (Scheme 5B) [31]. The palladium catalyzed Stille coupling [27] of **13** with *Z*-1-ethoxy-2-(tributylstannyl)ethene (**31**) followed by deprotection of the resulting enol ether, (*Z*)-6-amino-5-(2-ethoxyethenyl)-1*H*-pyrimidin-2-one (**32**), with concomitant cyclization, gave the novel XO prodrug substrate **16** (Scheme 5C).

The novel 5-chloro-6-[(2-iminopyrrolidin-1-yl)methyl]-3*H*-pyrimidin-4-one hydrochloride (**18**) was the only XO-activated prodrug of TPI to be synthesized (Scheme 6). The desulphurization of 6-methyl-2-thiouracil (**33**) by hydrogenolysis with an alkaline solution of Raney nickel gave 6-methyl-3*H*-pyrimidin-4-one (**34**) [32]. The chlorination of **34** at C-5 was achieved in high yield, by nucleophilic substitution with NCS in AcOH [33]. The resulting 5-chloro-6-methyl-3*H*-pyrimidin-4-one (**35**) was used to synthesize 5-chloro-6-(chloromethyl)-3*H*-pyrimidin-4-one (**36**) by radical halogenation using benzoyl peroxide and NCS. Subsequent coupling of **36** with 2-iminopyrrolidine hydrochloride (**37**) gave the TPI prodrug **18** (Scheme 6). The synthesis of the other proposed TPI prodrugs, **19** and **20** (see Scheme 3 for structures), by various methods were unsuccessful.

2.2. TP and XO enzymology

The enzymological evaluation of the TP inhibitors and XO-activated prodrugs with *E. coli* and human recombinant TP was determined by a continuous spectrophotometric assay [34,35]. The enzymological evaluation of substrate and prodrug activation by bovine XO, to determine the kinetic constants (K_m and V_{max}), were also determined using a continuous spectrophotometric assay [36] measuring the rate of product formed. The initial assays were carried out with *E. coli* TP and the potent inhibitors were further evaluated using the recombinant human enzyme.

The IC_{50} values of the competitive inhibitor 6A5BU with *E. coli* TP and human TP were 1.6 and 6.8 μM, respectively (Table 1). The literature IC_{50} values for 6A5BU were 30 μM with horse liver TP [8] and 17 μM with recombinant human TP [37]. The K_i value of 2.0 μM was determined, which compared well with the previously reported value of 0.80 μM [38]. The XO prodrug substrates, the 6-amino-5-bromopyrimidines **12**–**14**, displayed no inhibition of *E. coli* TP at high concentration (Table 1). Previous studies have shown that the imino and carbonyl moieties of the uracil ring are important for TP inhibition [13,39]. The lack of carbonyl substitution at C-2 and/or C-4 would therefore affect the acidity of N1–H and N3–H, in addition to preventing hydrogen-bonding interactions with the putative active site residues of TP. The IC_{50}

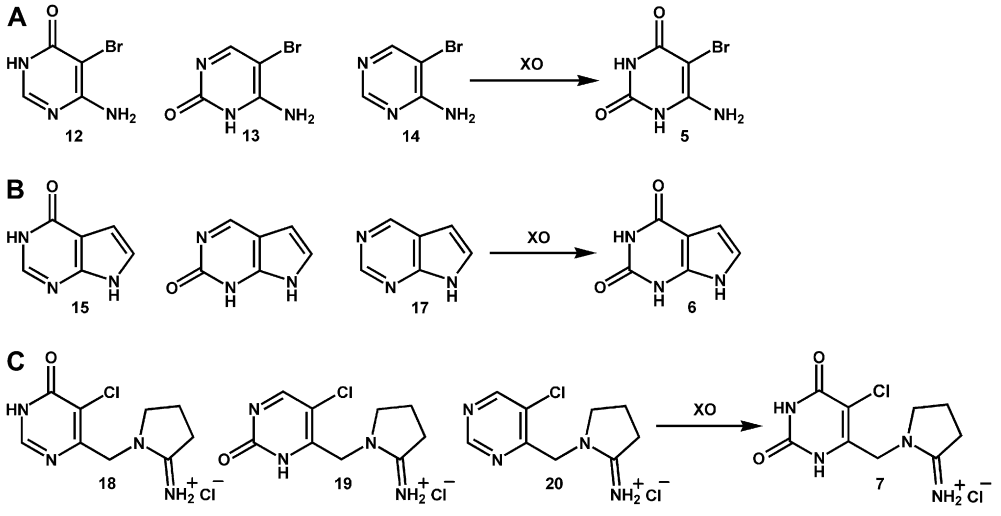

Scheme 3. Proposed oxidative prodrugs of TP inhibitors for XO-mediated biotransformation.

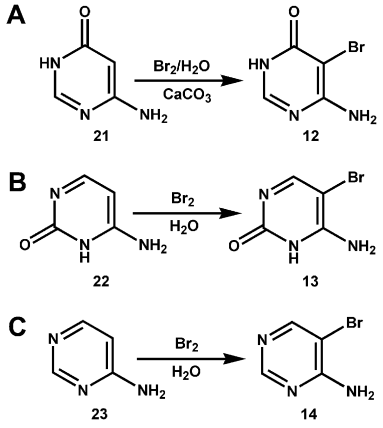

Scheme 4. The synthesis of 6-amino-5-bromopyrimidines (A) **12**, (B) **13** and (C) **14**.

data confirm that the 6-amino-5-bromopyrimidines are ideal candidates to evaluate the XO prodrug strategy. A comparative study of the specificities of XO and aldehyde oxidase (AO, EC 1.2.3.1) with a number of heterocyclic-based XO substrates [40] showed that the pyrimidine-based compounds, notably 4-aminopyrimidine and 4-hydroxy-6-aminopyrimidine, were good substrates for XO.

The XO-catalyzed rate of 6A5BU formation was evaluated for each 6-amino-5-bromopyrimidine over a concentration range (50–150 μM). The 6-amino-5-bromopyrimidines **12**–**14** were shown to be good substrates for XO (Table 1) and the formation of 6A5BU was observed in each case. The 6-amino-5-bromopyrimidine prodrug **12** displayed a K_m value with XO comparable to that of the natural substrate xanthine. From this data, the oxidation at the C-2 position of **12** is marginally favoured over that of the C-4 position of the 6-amino-5-bromopyrimidine **13**. The unsubstituted 6-amino-5-bromopyrimidine **14** had a lower affinity (higher K_m) for the enzyme and was oxidized at a slower rate by XO than the other 6-amino-5-bromopyrimidines, since **14** had to undergo two oxidations at C-2 and C-4 to form 6A5BU.

In the spectrophotometric assay, 7-DX (**6**) displayed modest inhibition of *E. coli* TP and human TP, with IC_{50} values of 6.5 and 45.0 μM, respectively, (Table 2). The 7*H*-pyrrolo[2,3-*d*]-pyrimidine XO prodrugs **15**–**17**, displayed no inhibition of TP at high concentration (Table 2). These 7*H*-pyrrolo[2,3-*d*]-pyrimidines further demonstrate the importance of the carbonyl substitution at the C-2 and C-4 positions in the uracil ring with regard to TP inhibition. The mercapto-substituted 7*H*-pyrrolo[2,3-*d*]pyrimidine compound **29**, exhibited 25% inhibition at 45 μM (Table 2), which may be a result of poor hydrogen-bonding interactions with the thione and the active site of TP, due to steric and electronic factors. The imidazo compound **24**, showed no TP inhibition at high concentration (Table 2), which again demonstrates the importance of the C-2 carbonyl and N1–H imino groups in the uracil ring system on TP inhibition. The natural substrate of XO, xanthine (**10**), was also evaluated producing 13% inhibition of TP at 158 μM (Table 2). The poor inhibition of **10** compared to 7-DX (**6**) was attributed to the poor binding of the hydrophilic fused-imidazole ring of **10**, in the hydrophobic region of the TP active site.

A comparative study [40] showed that **17** was a good substrate for XO. Another study that probed the active site of XO with a range of 7*H*-pyrrolo[2,3-*d*]pyrimidines [36] found that

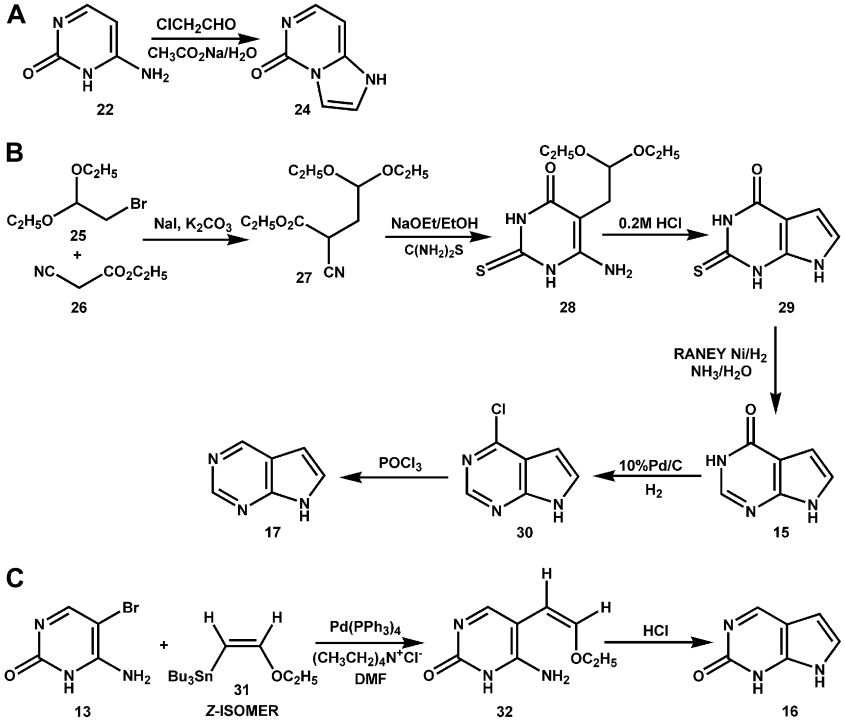

Scheme 5. The synthesis of (A) 6*H*-imidazo[1,2-*c*]pyrimidin-5-one (**24**) and the 7*H*-pyrrolo[2,3-*d*]pyrimidines (B) **15**, **17** and (C) **16**.

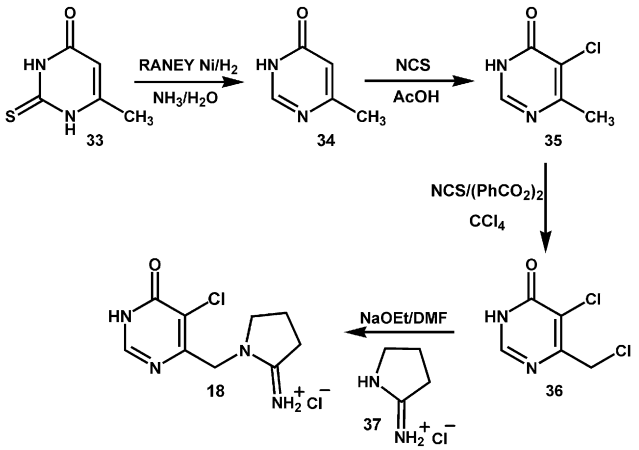

Scheme 6. The synthesis of 5-chloro-6-[(2-iminopyrrolidin-1-yl)methyl]-3*H*-pyrimidin-4-one hydrochloride (**18**).

15, the 7-deaza analogue of hypoxanthine, was oxidized exclusively at C-2 by XO, yielding 7-DX (**6**). In the aforementioned study, 7-DX displayed some inhibition of XO with hypoxanthine (K_i 25 μM) and xanthine (K_i 70 μM) as substrate [36], which supports the proposal that **15** acts as a prodrug for 7-DX activated by XO, and demonstrates that N-7 of the purine ring system is essential for enzymatic activation at C-8. In this study, the XO-catalyzed rate of 7-DX formation was evaluated for each 7*H*-pyrrolo[2,3-*d*]pyrimidine prodrug substrate over a concentration range (50–150 μM). The data confirmed that the 7*H*-pyrrolo[2,3-*d*]pyrimidines **15**–**17** act as prodrugs for XO generating 7-DX (Table 2). Prodrug **15** displayed kinetic constants of a similar magnitude to those reported [36]. The novel 7*H*-pyrrolo[2,3-*d*]pyrimidine **16** appeared to have a greater affinity for the XO active site than **15**, indicating that oxidation at the C-4 position is favoured over that of the C-2 position, in contrast to that found for the 6-amino-5-bromopyrimidines. However, 7*H*-pyrrolo[2,3-*d*]pyrimidine **17** had a lower affinity and was oxidized at a slower rate by XO than the other 7*H*-pyrrolo[2,3-*d*]pyrimidines, since oxidation at both C-2 and C-4 was required to form 7-DX. The replacement of the imidazole ring by a pyrrole moiety prevents oxidation at C-8 and no further oxidation of 7-DX was observed. The kinetic data of the 7*H*-pyrrolo[2,3-*d*]pyrimidines supports the finding that 7-DX is a competitive inhibitor of XO. 7-DX resembles the natural substrate xanthine in structure, binds to the active site of XO and competes with the appropriate 7*H*-pyrrolo[2,3-*d*]pyrimidine prodrug substrate. The competitive inhibition of 7-DX is supported by the significant low rate and increase in the K_m of the 7*H*-pyrrolo[2,3-*d*]pyrimidines in comparison with xanthine.

Table 1
The TP inhibition data for 6A5BU (**5**) and the 6-amino-5-bromopyrimidines **12**–**14** and the XO kinetic data for the 6-amino-5-bromopyrimidines **12**–**14**

Compound	*E. coli* TP IC_{50} (μM)	Human TP IC_{50} (μM)	Bovine XO K_m (μM)	Bovine XO V_{max} (μM/min)
5	1.6 ± 0.17	6.8 ± 0.7	–	–
12	73.7–147.7 No inhibition	–	23.8	1.253
13	68.4–136.9 No inhibition	–	32.5	1.198
14	106.3–212.6 No inhibition	–	44.4	0.982

Table 2
The TP inhibition data for 7-DX (**6**) and the 7*H*-pyrrolo[2,3-*d*]pyrimidines **15**–**17** and **29**, xanthine (**10**), and 6*H*-imidazo[1,2-*c*]pyrimidin-5-one (**24**) and the XO kinetic data for xanthine (**10**) and the 7*H*-pyrrolo[2,3-*d*]pyrimidines **15**–**17**

Compound	*E. coli* TP IC_{50} (μM)	Human TP IC_{50} (μM)	Bovine XO K_m (μM)	Bovine XO V_{max} (μM/min)
6	6.5 ± 0.92	45.0 ± 7.0	–	–
15	No inhibition at 103.6–207.2	–	45.1	0.507
16	No inhibition at 74.0–148.0	–	29.8	0.484
17	No inhibition at 81.4–162.8	–	67.2	0.242
10	13% inhibition at 158.0	–	21.4	2.768
24	No inhibition at 163.0	–	–	–
29	25% inhibition at 45.0	–	–	–

The TP inhibitor, TPI (**7**) was evaluated by the spectrophotometric method with *E. coli* and human TP to give IC_{50} values of 20 and 23 nM, respectively. A previous study reported an IC_{50} value of 35 nM for TPI with human TP using a [^{3}H]thymidine assay and a K_i of 20 nM [11]. The halogen substitution at the C-5 position of the uracil ring confers significant TP inhibition. The increased acidity of the uracil N1–H and N3–H groups within these compounds promotes the oxyanion character of the carbonyl substituents at C-2 and C-4, through the electron-withdrawing halogen group, resulting in strong hydrogen-bonding interactions of the uracil anion with residues in the active site of TP. The resemblance of TPI to the zwitterionic transition state proposed for thymidine phosphorolysis (Scheme 1) explains the high potency of TPI, which has been shown to inhibit TP in a tight-binding stoichiometric manner [34].

The TPI prodrug **18** displayed no inhibition of *E. coli* or human TP at high concentration (Table 3). This lack of inhibition further highlights the importance of the C-2 carbonyl group in the uracil ring system. Therefore compound **18** would be an ideal potential TPI prodrug substrate for XO, with a large TP inhibition selectivity ratio. The selective oxidation at C-2 in the uracil ring system of **18** by XO results in the formation of TPI. In addition, the synthetic intermediate 5-chloro-6-methyl-3*H*-pyrimidin-4-one (**35**) displayed no inhibition of *E. coli* TP at 66.0 μM, again demonstrating the importance of the C-2 carbonyl group in the uracil ring system with respect to TP inhibition.

The XO-catalyzed rate of TPI formation was evaluated for the prodrug substrate **18** over a concentration range (50–150 μM). In comparison to xanthine and the 6-amino-5-bromopyrimidines, the prodrug substrate **18** displayed a high K_m value of 64.9 μM, indicative of a low affinity for the XO active site. This was reflected in a low turnover rate, which was surprising for a pyrimidin-2-one ring based compound with one site available for oxidation, especially at the C-2 position, which appears

Table 3
The TP inhibition data for TPI (**7**), 5-chloro-6-methyl-3*H*-pyrimidin-4-one (**35**) and 5-chloro-6-[1-(2-iminopyrrolidinyl)methyl]-3*H*-pyrimidin-4-one (**18**) and the XO kinetic data for (**18**)

Compound	*E. coli* TP IC_{50} (μM)	Human TP IC_{50} (μM)	Bovine XO K_m (μM)	Bovine XO V_{max} (μM/min)
7	0.02 ± 0.0018	0.023 ± 0.0045	–	–
35	No inhibition at 66.0	–	–	–
18	No inhibition at 47.2	No inhibition at 62.3	64.9	0.510

to be favoured in the 6-amino-5-bromopyrimidine series. The poor XO-catalyzed oxidation rate was probably due to the presence of the cationic 2-iminopyrrolidine ring system, although tolerated by XO is perhaps not sterically or electronically preferred. However, TPI (**7**) formation was observed, with the prodrug **18** being oxidized at the C-2 position by XO (Table 3).

2.3. Molecular modelling with human TP

To provide explanation for the differences in TP inhibition for the TP inhibitors and XO prodrugs, the interactions between the small molecule ligands and the protein were modelled. The optimal TP-ligand geometries were predicted using energy minimization with the Tripos force field [41], from the compounds modelled into the active site of the crystallographic structure of human TP [42]. 6A5BU (**5**) displays hydrogen-bonding interactions with His116, Arg202, Ser217 and Lys221 in the human TP crystal structure, the bromine atom at C-5 is anchored in a hydrophobic pocket formed by the Val208 and Ile214 residues of the α-domain and the Leu148 and Val241 residues of the α/β-domain and the amino group at C-6, of 6A5BU, interacts with both Ser117 and Thr118 (Table 4). The absence of the C-2 and/or C-4 carbonyl group in the 6-amino-5-bromopyrimidines **12**–**14** effects the extent of binding to key amino acid residues and as a result the orientation of the pyrimidine ring in the TP active site: the 5-bromo-3*H*-pyrimidin-4-one ring of **12** displays hydrogen-bonding interactions with Arg202 and Ser217, however, no interactions were observed with His116 and Lys221, due to lack of substitution at C-2, which prevents stabilization of the pyrimidine ring in the active site. The 5-bromo-1*H*-pyrimidin-2-one ring of **13** displays hydrogen-bonding interactions with His116, Arg202 and Lys221 and no interaction was observed with Ser217, the N-3 imine of the pyrimidine ring hydrogen-bonds with Arg202, since the 4-oxo group is absent in **13**, which elevates the pyrimidine ring towards the Ile214 and Ser217 residues. The 5-bromopyrimidine ring of **14** exhibits hydrogen-bonding between the N-3 imine of the pyrimidine ring and Lys221, altering the position of the pyrimidine binding compared to that of 6A5BU. In all of the 6-amino-5-bromopyrimidine prodrugs examined, the amino group at C-6 interacts with Ser117, but no hydrogen-bonding interaction was observed with Thr118 as in 6A5BU, due to distorted pyrimidine ring binding (Table 4). The lack of C-2 and/or C-4 carbonyl groups in the pyrimidine ring reduces the interactions with active site residues and results in poor binding in the active site of TP.

Table 4
The interactions and calculated hydrogen-bond distances of the TP inhibitors and XO prodrugs with human TP

Compound	Hydrogen bond interaction		Hydrogen bond distance (Å)
	Amino acid	Ligand	
5	His116	N1–H	2.39
	Ser117	NH_2	2.74
	Thr118	NH_2	1.93
	Arg202	O4	1.87, 1.96
	Ser217	N3–H	1.80
	Lys221	O2	1.83
12	Ser117	NH_2	2.10
	Arg202	O4	1.72, 2.12
	Ser217	N3–H	1.81
13	His116	N1–H	2.78
	Ser117	NH_2	2.43
	Arg202	N3	2.48
	Lys221	O2	1.71, 2.65
14	Ser117	NH_2	2.62
	Ser217	N3	1.66, 1.76
6	His116	N1–H	2.24
	Ser117	N7–H	2.72
	Arg202	O4	1.85, 1.89
	Ser217	N3–H	1.69
	Lys221	O2	1.83, 2.74
15	Ser117	N7–H	2.66
	Arg202	O4	1.81, 1.82
	Ser217	N3–H	1.84
16	His116	N1–H	2.63
	Lys221	O2	2.77
17	Lys221	N3	1.96
7	His116	N1–H	2.86
	Ser117	NH_2^+	1.69
	Arg202	O4	1.89, 1.94
	Ser217	N3–H	1.74
	Lys221	O2	1.91
18	Ser117	NH_2^+	1.72
	Arg202	O4	1.78, 1.81
	Ser217	N3–H	1.86

The uracil ring moiety of 7-DX (**6**) makes hydrogen-bonding interactions with His116, Arg202, Ser217 and Lys221 residues in the TP active site (Fig. 2A). The N7–H imino group of the pyrrole moiety of 7-DX forms hydrogen-bonds with Ser117 and the hydrophobic pocket accommodates the ethenyl group. The pyrimidin-4(3*H*)-one ring of **15** exhibits hydrogen-bonding interactions with Arg202 and Ser217 (Fig. 2B). No interactions were observed with His116 and Lys221, due to the lack of substitution at C-2. As a consequence, **15** appears to be raised towards the hydrophobic pocket and is supported by the shorter hydrogen-bond distances between the 4-oxo group of the pyrimidine ring and the longer hydrogen-bond distance between N7–H and Ser117 compared to 7-DX. The pyrimidin-4(3*H*)-one ring of **16** displays hydrogen-bonding interactions with His116 and Lys221 and no interactions were observed with Ser117, Arg202 or Ser217 (Fig. 2C). The pyrimidine ring system of **17** exhibits hydrogen-bonding between the N-3 imine and Lys221, allowing the pyrrole moiety to face the hydrophobic pocket (Fig. 2D). The lack of C-2

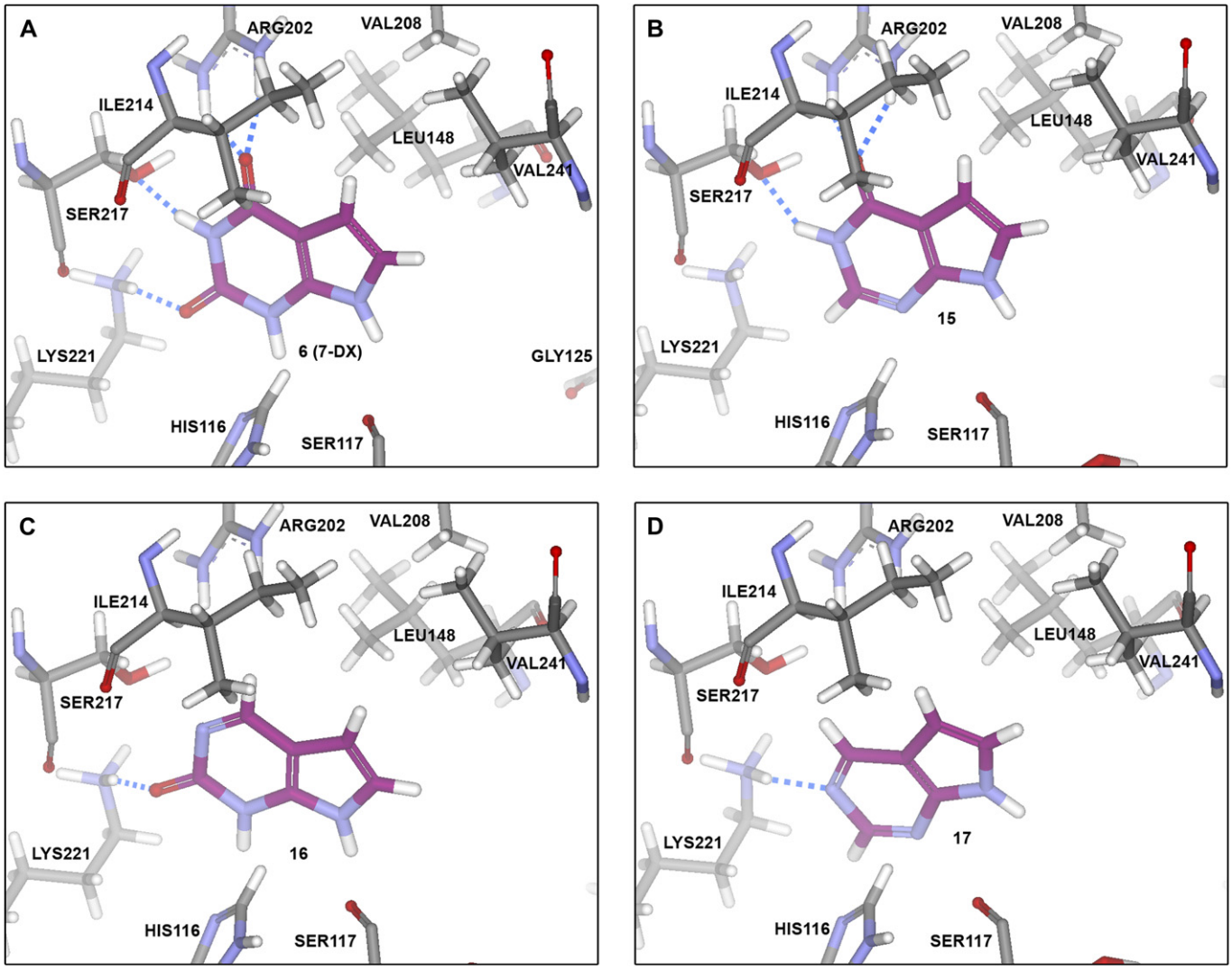

Fig. 2. Representations of the key interactions of (A) 7-DX (**6**) and the 7*H*-pyrrolo[2,3-*d*]pyrimidines (B) **15**, (C) **16** and (D) **17** with the active site of human TP. Figures display hydrogen-bond contacts (blue dashed lines) between the ligand and amino acid residues (coloured by atom type, except ligand carbons atoms which are coloured purple). The figures were constructed using Discovery Studio Viewer Professional Software (Accelrys, Inc., San Diego, CA). (For interpretation of the references to color in this figure legend, the reader is referred to the web version of this article.)

and/or C-4 substitution in the 7*H*-pyrrolo[2,3-*d*]pyrimidines **15**–**17**, results in reduced hydrogen-bonding interactions with active site residues (Table 4) and affords explanation for the absence of TP inhibition at high concentration.

The uracil ring system of TPI (**7**) makes a number of hydrogen-bonding interactions with His116, Arg202, Ser217 and Lys221. The C-5 chlorine atom occupies the hydrophobic pocket formed by Val208, Ile214, Leu148 and Val241 and the 2-iminopyrrolidinyl ring moiety lies perpendicular to the plane of the uracil ring and allows the amino group to interact with Ser117 (Fig. 3A). The absence of C-2 carbonyl in the TPI prodrug, **18**, affects the binding interaction and orientation of the pyrimidin-4-one ring in the active site of TP. The 5-chloro-3*H*-pyrimidin-4-one ring of **18** displays hydrogen-bonding interactions with Arg202 and Ser217, however, no hydrogen-bonding interactions with His116 or Lys221 were observed, due to lack of substitution at C-2 (Fig. 3B). The 5-chloro-3*H*-pyrimidin-4-one moiety of **18** appears to be raised towards the hydrophobic pocket and this observation is supported by the shorter hydrogen-bond distances between the 4-oxo group of the 5-chloro-3*H*-pyrimidin-4-one moiety and the Arg202 residue, and the longer hydrogen-bond distance between the amino group of the 2-iminopyrrolidinyl and the Ser117 residue, compared to the equivalent interactions with TPI (Table 4). The conformation of the 2-iminopyrrolidinyl ring appears unchanged in TPI and **18**. The lack of C-2 substitution in the pyrimidin-4-one ring of **18** reduced the interaction with active site residues and as a result no inhibition of TP was achieved with **18** at high concentration.

3. Conclusion

In this article, we have described the XO-mediated oxidation of a series of prodrug compounds generating the appropriate TP inhibitor. The 6-amino-5-bromopyrimidines **12**–**14**, prodrugs of the TP inhibitor 6A5BU (**5**), were synthesized

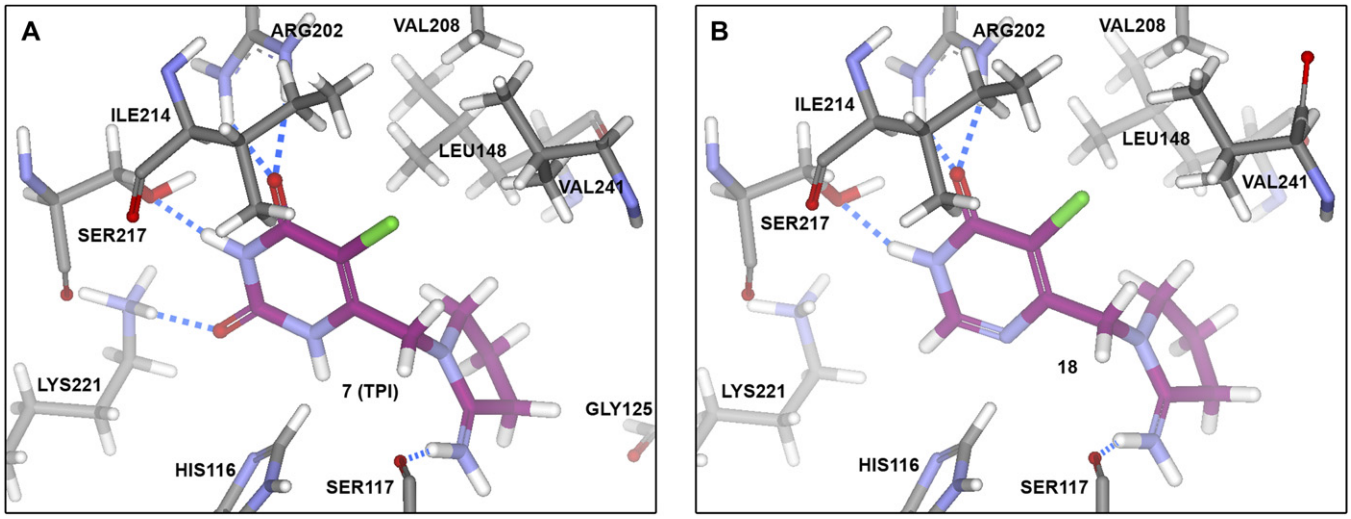

Fig. 3. Representations of the key interactions of (A) TPI (**7**) and (B) 5-chloro-6-[1-(2-iminopyrrolidinyl)methyl]-3*H*-pyrimidin-4-one (**18**) with the active site of human TP. Figures display hydrogen-bond contacts (blue dashed lines) between the ligand and amino acid residues (coloured by atom type, except ligand carbons atoms which are coloured purple). The figures were constructed using Discovery Studio Viewer Professional Software (Accelrys, Inc., San Diego, CA). (For interpretation of the references to color in this figure legend, the reader is referred to the web version of this article.)

and displayed no inhibition of *E. coli* TP at high concentrations. Molecular modelling confirmed that the C-2 and C-4 carbonyl groups of the uracil ring are essential for TP inhibition. The 6-amino-5-bromopyrimidine prodrugs were all oxidized at an appreciable rate by XO, forming 6A5BU. The 7*H*-pyrrolo[2,3-*d*]pyrimidines **15**–**17**, prodrugs of 7-DX (**6**), were synthesized and displayed no inhibition of *E. coli* TP at high concentration, further demonstrating the importance of the C-2 and C-4 carbonyl groups of the uracil moiety on TP inhibition. This was supported by molecular modelling studies, where fewer hydrogen-bonding interactions were observed between the 7*H*-pyrrolo[2,3-*d*]pyrimidines and the TP active site. The 7*H*-pyrrolo[2,3-*d*]pyrimidine prodrugs were all oxidized by XO, albeit at a slow rate, forming 7-DX without further oxidation. 5-Chloro-6-[1-(2-iminopyrrolidinyl)methyl]pyrimidine (**18**), a prodrug of TPI (**7**), lacking the C-2 carbonyl, displayed no inhibition of *E. coli* or human TP. This was supported by molecular modelling studies, where no hydrogen-bonding was observed with Lys221 or His116, which suggests that the 1-amido group of the uracil ring is essential for TP inhibition. The prodrug substrate **18** was selectively oxidized at C-2, at a slow rate by XO, yielding TPI. The prodrugs may be useful in assisting the oral delivery of TP inhibitors by improving solubility, bioavailability and tumour selectivity.

4. Experimental

4.1. Materials and instrumentation

Chemicals and reagents were obtained from the Sigma-Aldrich Chemical Co. Dorset, UK and Lancaster Synthesis Ltd. Lancashire, UK. Silica gel 33–70 μm, 200–400 mesh, pH 6.5–7.5, for column chromatography were obtained from BDH, VWR International, Leicestershire, UK. Deuterated solvents (DMSO-d_6, D_2O and $CDCl_3$) and tetramethylsilane (TMS) were supplied by Cambridge Isotope Laboratories Inc., Andover, USA. Xanthine oxidase (X4376, 0.4 unit/mg protein, one unit will convert 1.0 μmol of xanthine to uric acid per minute at pH 7.5 at 25 °C) from buttermilk, recombinant *E. coli* thymidine phosphorylase (T2807, 1060 units/ml, one unit will convert 1.0 μmol each of thymidine and phosphate to thymine and 2-deoxyribose-1-phosphate per minute at pH 7.4 at 25 °C) and recombinant human thymidine phosphorylase (T9319, 9–10 unit/mg protein, one unit will form 1 nmol thymine per minute at pH 7.0 at 37 °C), expressed in V79 Chinese hamster cells, were obtained from the Sigma-Aldrich Chemical Co. Dorset, UK.

Analytical thin-layer chromatography (TLC) was performed on Merck pre-coated silica gel 60 F_{254} plates and visualized by ultra-violet illumination (254 nm) using a UV GL-58 mineral-light lamp. Melting points (m.pt.) were determined in open glass capillary tubes on Gallenkamp M.P.D.350.BM2.5 micromelting point apparatus and are uncorrected. Nuclear magnetic resonance (NMR) spectra were recorded on a 300 MHz Bruker Avance 300 spectrometer. ^{1}H NMR spectra were recorded in δ_H parts per million (ppm) in DMSO-d_6 or $CDCl_3$ with TMS as the reference. The coupling constants (J) are expressed in Hertz (Hz). ^{13}C NMR spectra were recorded in δ_C parts per million (ppm) in DMSO-d_6 or $CDCl_3$ with TMS and the solvent peak as internal standards, ^{13}C DEPT-135 NMR spectra confirmed assignment. Infra-red (IR) spectra were recorded on a Satellite FTIR Mattson spectrometer, with Mattson WinFIRST software. The samples were prepared on a Specac golden gate single reflection ATI system. Ultra-violet (UV) spectra were recorded on a Unicam UV 300 spectrophotometer, with Thermospectronic Vision 32 software, using Hellma UV quartz cuvettes, for compound analysis and for XO enzyme kinetics. A Molecular Devices SpectraMax M2 UV–visible spectrophotometer, with SoftMax Pro software, using a 96-well microplate was used for TP enzyme kinetics. Mass spectra and elemental analysis

were determined at the Department of Chemistry, University of Manchester. Electron ionization and positive and negative chemical ionization mass spectra were recorded on an automated Fisons TRIO 2000 quadrapole spectrometer. Both positive and negative electrospray (ES) ionization and atmospheric pressure chemical ionization (APCI) mass spectra were recorded using a Micromass Platform II atmospheric pressure ionization spectrometer coupled to an HPLC system.

4.2. Chemistry

6-Amino-5-bromouracil (6A5BU, **5**) was prepared from 6-aminouracil and NBS [43]. 7-Deazaxanthine (7-DX, **6**) was prepared from 6-amino-2,4-hydroxypyrimidine and chloroacetaldehyde [28]. Ethyl 2-cyano-4,4-diethoxybutanoate (**27**) was prepared from bromoacetaldehyde diethyl acetal (**25**) and ethyl cyanoacetate (**26**) in the presence of K_2CO_3 and sodium iodide [31]. 5-Chloro-6-[1-(2-iminopyrrolidinyl)methyl]uracil hydrochloride (TPI, **7**) [10] was prepared by the reaction of 5-chloro-6-(chloromethyl)uracil [44] and 2-iminopyrrolidine hydrochloride [45] in the presence of sodium ethoxide. (*Z*)-1-Ethoxy-2-(tributylstannyl)ethene (**31**) was prepared from tributyltin hydride, ethoxyacetylene and $PdCl_2(PPh_3)_2$ [46]. 6-Amino-5-(2,2-diethoxyethyl)-2-thiouracil (**28**) was prepared by the reaction of thiourea with ethyl 2-cyano-4,4-diethoxybutanoate [30]. 2-Mercapto-7*H*-pyrrolo[2,3-*d*]pyrimidin-4(3*H*)-one (**29**) was prepared by the reaction of 6-amino-5-(2,2-diethoxyethyl)-2-thiouracil with HCl [30]. 6-Methyl-3*H*-pyrimidin-4-one (**34**) was prepared by the reaction of 6-methyl-2-thiouracil (10.0 g, 70.3 mmol, 1 eq) with Raney nickel [32].

4.2.1. 6-Amino-5-bromo-3H-pyrimidin-4-one (*12*)

Bromine (0.87 ml, 16.9 mmol, 1.25 eq) was added dropwise to a stirred suspension of 6-amino-4-hydroxypyrimidine (1.50 g, 13.5 mmol, 1 eq) in water (20 ml). The reaction mixture was stirred for 1 h at room temperature. The solution was then made alkaline with 20% aqueous K_2CO_3 (pH ~ 9) and a white precipitate was formed. The reaction mixture was filtered giving a colourless solid, which was recrystallized from water and vacuum-dried. The title compound **12** was isolated as a white powder (1.21 g, 47.3%). TLC R_f 0.57 (1:1, MeOH/DCM); m.pt. 266.5–267.5 °C, m.pt. [26] 268.0 °C; ^{1}H NMR (DMSO-d_6) δ: 6.75 (2H, br s, NH_2), 7.82 (1H, s, C2–H), 10.5 (1H, br s, N3–H); ^{13}C NMR (DMSO-d_6) δ: 82.7 (C-5), 147.7 (C-2), 157.7 (C-6), 160.4 (C-4); MS (ES+) 190 (^{79}Br M + H, 95%), 192 (^{81}Br M + H, 93%). Elemental analysis: $C_4H_4BrN_3O$, calculated (%): C 25.29, H 2.12, N 22.12, Br 42.06. Found (%): C 25.21, H 2.08, N 22.04, Br 41.97.

4.2.2. 6-Amino-5-bromo-1H-pyrimidin-2-one (*13*)

6-Amino-5-bromo-1*H*-pyrimidin-2-one was prepared as described for **12** using 6-amino-2-hydroxypyrimidine (4.0 g, 36.0 mmol, 1 eq) as starting material to give the product **13** as a colourless powder (3.83 g, 56.0%). TLC R_f 0.58 (1:1, MeOH/DCM); m.pt. 241.5–242.5 °C, m.pt. [26] 240–242 °C; ^{1}H NMR (DMSO-d_6) δ: 6.85 (2H, br s, NH_2), 7.76 (1H, s, C4–H), 10.5 (1H, br s, N1–H); ^{13}C NMR (DMSO-d_6) δ: 85.1 (C-5), 144.1 (C-4), 155.2 (C-6), 162.5 (C-2); MS (ES+) 190 (^{79}Br M + H, 100%), 192 (^{81}Br M + H, 94%). Elemental analysis: $C_4H_4BrN_3O$, calculated (%): C 25.29, H 2.12, N 22.12, Br 42.06. Found (%): C 24.97, H 1.98, N 21.33, Br 42.15.

4.2.3. 6-Amino-5-bromopyrimidine (*14*)

Bromine (1.58 ml, 30.8 mmol, 1.95 eq) was added dropwise to a mixture of 6-amino-pyrimidine (1.50 g, 15.8 mmol, 1 eq), $CaCO_3$ (0.39 g, 3.9 mmol, 0.25 eq) and water (20 ml) and stirred for 30 min at 55–60 °C. The solution was made alkaline with 20% aqueous K_2CO_3 (pH ~ 9) and extracted with EtOAc (2 × 100 ml). The EtOAc layer was dried over K_2CO_3, filtered and then reduced to dryness *in vacuo*, giving a yellow coloured residue, which was purified by Al_2O_3 column chromatography using EtOAc as eluent. The required fractions were collected, pooled and reduced to dryness *in vacuo*, the residue was recrystallized from methanol and vacuum-dried to give the title compound **14** as a colourless powder (1.46 g, 53.1%). TLC R_f 0.60 (1:1, MeOH/DCM); m.pt. 208.5–209.5 °C, m.pt. [27] 208–210 °C; ^{1}H NMR (DMSO-d_6) δ: 8.32 (2H, s, C2–H and C4–H), 7.25 (2H, br s, NH_2); ^{1}H NMR ($CDCl_3$) δ: 7.05 (2H, br s, NH_2), 8.40 (1H, s, C4–H), 8.47 (1H, s, C2–H); ^{13}C NMR (DMSO-d_6) δ: 102.4 (C-5), 156.0 (C-2), 156.7 (C-4), 160.0 (C-6); MS (APCI+) 174 (^{79}Br M + H, 100%), 176 (^{81}Br M + H, 97%). Elemental analysis: $C_4H_4BrN_3$, calculated (%): C 27.61, H 2.32, N 24.15, Br 45.92. Found (%): C 27.43, H 2.42, N 23.98, Br 45.99.

4.2.4. 7H-Pyrrolo[2,3-d]pyrimidin-4(3H)-one (*15*)

7*H*-Pyrrolo[2,3-*d*]pyrimidin-4(3*H*)-one was prepared by an adaptation of a known procedure [30]. Concentrated aqueous ammonia (40 ml) was added to a suspension of 2-mercapto-7*H*-pyrrolo[2,3-*d*]pyrimidin-4(3*H*)-one (15.0 g, 89.7 mmol, 1 eq) in water (100 ml). The solution was stirred at 50 °C and Raney nickel (75 ml, slurry in water) was added portion-wise. The reaction mixture was then heated at reflux for 3 h then the catalyst was removed by filtration. The filtrate was evaporated to dryness *in vacuo* and the resulting precipitate was collected by filtration, washed serially with water, methanol and ether, and vacuum-dried to provide the title compound **15** as a colourless powder (9.82 g, 81.0%). TLC R_f 0.55 (4:1, EtOAc/MeOH); m.pt. > 320 °C, m.pt. [30] 340–345 °C; ^{1}H NMR (DMSO-d_6) δ: 6.45 (1H, d, $^3J_{HH}$ = 3.3 Hz, C5–H), 7.04 (1H, d, $^3J_{HH}$ = 3.2 Hz, C6–H), 7.84 (1H, s, C2–H), 11.78 (1H, s, N7–H), 11.86 (1H, s, N3–H); ^{13}C NMR (DMSO-d_6) δ: 101.9 (C-5), 107.6 (C-9), 120.3 (C-6), 143.1 (C-2), 148.0, (C-8), 158.4 (C-4); IR: 1710 cm^{-1} (C=O), 3470 cm^{-1} (N–H); MS: (APCI+) 136 (M + H, 100%), (APCI−) 134 (M − H, 100%). Elemental analysis: $C_6H_5N_3O$, calculated (%): C 53.33, H 3.73, N 31.10. Found (%): C 53.31, H 3.62, N 30.50.

4.2.5. 4-Chloro-7H-pyrrolo[2,3-d]pyrimidine (*30*)

4-Chloro-7*H*-pyrrolo[2,3-*d*]pyrimidine was prepared by an adaptation of a known procedure [31]. A mixture of 7*H*-pyrrolo[2,3-*d*]pyrimidin-4(3*H*)-one (1.35 g, 10.0 mmol, 1 eq)

and $POCl_3$ (15 ml, 160.9 mmol, 16 eq) was stirred for 1 h with heating at reflux. Excess $POCl_3$ was removed under vacuum then dichloromethane (200 ml) and iced water (100 ml) were added and the mixture stirred until the black solid dissolved. The organic layer was separated, washed with bicarbonate solution, dried over $MgSO_4$ and then evaporated to dryness *in vacuo*. The yellow residue was recrystallized (1:1, v/v, toluene/hexane) to give pure **30** as fine colourless needles (1.02 g, 65.6%). TLC R_f 0.68 (4:1, EtOAc/hexane); m.pt. 186–188 °C, m.pt. [31] 188–190 °C; ^{1}H NMR (DMSO-d_6) δ: 6.62 (1H, d, $^3J_{HH} = 3.2$ Hz, C5–H), 7.71 (1H, d, $^3J_{HH} = 3.2$ Hz, C6–H), 8.60 (1H, s, C2–H), 12.58 (1H, s, N7–H); ^{13}C NMR (DMSO-d_6) δ: 98.7 (C-5), 116.5 (C-9), 128.3 (C-6), 150.2 (C-8), 150.4, (C-2), 151.7 (C-4); MS: (APCI+) 154 (^{35}Cl M^+, 20%), (APCI−) 152 (^{35}Cl M^-, 100%). Elemental analysis: $C_6H_4ClN_3$, calculated (%): C 46.93, H 2.63, N 27.36, Cl 23.09. Found (%): C 47.39, H 2.32, N 26.41, Cl 23.54.

4.2.6. 7H-Pyrrolo[2,3-d]pyrimidine (17)

7*H*-Pyrrolo[2,3-*d*]pyrimidine was prepared by an adaptation of a known procedure [31]. A solution of 4-chloro-7*H*-pyrrolo[2,3-*d*]pyrimidine (0.12 g, 0.8 mmol, 1 eq) in ethanol (20 ml) and concentrated aqueous NH_3 (0.5 ml, 6.6 mmol, 8.25 eq) and 10% Pd/C (0.04 g) was stirred in a H_2 atmosphere for 6 h at room temperature. The catalyst was removed by filtration and the solvent was evaporated. The residue was washed with H_2O, filtered and dried under high vacuum giving the title compound **17** as a fine colourless powder (0.08 g, 83.7%). TLC R_f 0.62 (4:1, EtOAc/MeOH); m.pt. 129–130 °C, m.pt. [31] 131–133 °C; ^{1}H NMR (DMSO-d_6) δ: 6.61 (1H, d, $^3J_{HH} = 3.5$ Hz, C5–H), 7.59 (1H, d, $^3J_{HH} = 3.5$ Hz, C6–H), 8.77 (1H, s, C4–H), 9.02 (1H, s, C2–H), 12.26 (1H, s, N7–H); ^{13}C NMR (DMSO-d_6) δ: 99.3 (C-5), 118.1 (C-9), 127.2 (C-6), 148.7 (C-8), 150.7, (C-2), 151.0 (C-4); IR: 3450 cm^{-1} (N–H); MS: (APCI+) 120 (M + H, 100%). Elemental analysis: $C_6H_5N_3$, calculated (%): C 60.50, H 4.23, N 35.27. Found (%): C 59.26, H 5.29, N 34.16.

4.2.7. (Z)-6-Amino-5-(2-ethoxyethenyl)-1H-pyrimidin-2-one (32)

A mixture of 6-amino-5-bromo-1*H*-pyrimidin-2-one (0.95 g, 5.0 mmol, 1 eq), (*Z*)-1-ethoxy-2-(tributylstannyl)ethene (2.17 g, 6.0 mmol, 1.2 eq), tetraethylammonium chloride (0.92 g, 5.0 mmol, 1 eq) and $PdCl_2(PPh_3)_2$ (140 mg, 0.2 mmol, 0.04 eq) in DMF (20 ml) was heated at reflux for 5 h. The reaction mixture was reduced to dryness *in vacuo*, giving a brown coloured residue and purified by fractionation through a short silica gel column (4:1, v/v, EtOAc/hexane), the required fractions were pooled and evaporated, recrystallization from ethanol gave compound **32** as a beige powder (0.58 g, 64.0%). TLC R_f 0.49 (4:1, EtOAc/MeOH); m.pt. 89.5–90 °C; ^{1}H NMR (DMSO-d_6) δ: 1.27 (3H, t, $J = 7.2$ Hz, $-CH_2-CH_3$), 4.07 (2H, q, $J = 7.2$ Hz, CH_2-CH_3), 5.28 (1H, d, $^3J_{HH} = 7.0$ Hz, C1′–H), 6.42 (1H, d, $^3J_{HH} = 7.0$ Hz, C2′–H), 7.50 (1H, s, C4–H), 6.48 (2H, s, NH_2), 10.42 (1H, s, N1–H); ^{13}C NMR (DMSO-d_6) δ: 14.8 (CH_3), 63.1 (CH_2), 85.1 (C2′–H), 99.8 (C-5), 145.2 (C1′–H), 145.4 (C-6) 160.7 (C-2), 163.7 (C-4); MS: (APCI+) 182 (M + H, 100%), (APCI−) 180 (M − H, 100%).

4.2.8. 7H-Pyrrolo[2,3-d]pyrimidin-2(1H)-one (16)

A solution of (*Z*)-6-amino-5-(2-ethoxyethenyl)-1*H*-pyrimidin-2-one (0.50 g, 2.76 mmol, 1 eq) and concentrated HCl (3.0 ml) in water (20 ml) was heated at reflux for 30 min. The solution was evaporated and the residue was made alkaline (pH ~ 9) with aqueous 20% K_2CO_3 and extracted with EtOAc (2 × 75 ml). The solvent was removed by distillation under reduced pressure and the resulting precipitate was collected by filtration, washed serially with water and ethanol, and vacuum-dried to provide the title compound **16** as a beige powder (0.37 g, 85.0%). TLC R_f 0.54 (4:1, EtOAc/MeOH); m.pt. 159–160 °C; ^{1}H NMR (DMSO-d_6) δ: 6.46 (1H, d, $^3J_{HH} = 3.3$ Hz, C5–H), 7.04 (1H, d, $^3J_{HH} = 3.3$ Hz, C6–H), 8.47 (1H, s, C4–H), 11.80 (1H, s, N1–H), 11.85 (1H, s, N7–H); ^{13}C NMR (DMSO-d_6) δ: 101.7 (C-5), 107.6 (C-9), 120.3 (C-6), 143.1 (C-8), 148.0 (C-2), 158.4 (C-4); IR: 1710 cm^{-1} (C=O), 3450 cm^{-1} (N–H); MS: (APCI+) 136 (M + H, 100%), (APCI−) 134 (M − H, 100%). Elemental analysis: $C_6H_5N_3O$, calculated (%): C 53.33, H 3.73, N 31.10. Found (%): C 53.08, H 3.56, N 30.51.

4.2.9. 6H-Imidazo[1,2-c]pyrimidin-5-one (24)

Chloroacetaldehyde (50%, v/v, solution in water, 1.4 ml, 10.8 mmol, 1.2 eq) was added dropwise to a stirred mixture of 6-amino-1*H*-pyrimidin-2-one (1.0 g, 9.0 mmol, 1 eq) in DMF (6.0 ml) at 50 °C. A colour change of white to pink was observed after the addition of chloroacetaldehyde. The reaction mixture was heated at 50 °C for 12 h. The solvent was removed by distillation under reduced pressure and the resulting precipitate was collected by filtration, washed serially with ethanol and ether, and dried to provide the title compound **24** as a beige powder (0.91 g, 74.7%). TLC R_f 0.45 (4:1, EtOAc/MeOH); m.pt. 278.0–278.5 °C, m.pt. [29] 272–274 °C; ^{1}H NMR (DMSO-d_6) δ: 6.87 (1H, d, $^3J_{HH} = 7.4$ Hz, C8–H), 7.79 (1H, d, $^3J_{HH} = 7.4$ Hz, C7–H), 7.92 (1H, d, $^3J_{HH} = 2.2$ Hz, C3–H), 8.10 (1H, d, $^3J_{HH} = 2.2$ Hz, C2–H), 12.72 (1H, br s, N6–H); ^{13}C NMR (DMSO-d_6) δ: 93.7 (C-3), 115.0 (C-7), 123.8 (C-2), 138.8 (C-8), 145.6 (C-9), 145.9 (C-5); IR: 1720 cm^{-1} (C=O), 3340 cm^{-1} (N–H); MS: (ES+) 136 (M + H, 60%), (ES−) 134 (M − H, 100%). Elemental analysis: $C_6H_5N_3O$, calculated (%): C 53.33, H 3.73, N 31.10. Found (%): C 53.15, H 3.67, N 30.96.

4.2.10. 5-Chloro-6-methyl-3H-pyrimidin-4-one (35)

A mixture of 6-methyl-3*H*-pyrimidin-4-one (5.0 g, 45.4 mmol, 1 eq) in glacial AcOH (100 ml) was heated to 80 °C until the solid dissolved. The mixture was cooled to 60 °C and NCS (6.67 g, 49.9 mmol, 1.1 eq) was added. The reaction mixture was heated at reflux for 5 h. The reaction mixture was evaporated to dryness *in vacuo*, the residue was treated with a minimum amount of water and placed in the refrigerator at 5 °C overnight. A colourless precipitate formed

was collected by filtration. The solid was vacuum-dried giving **35** as a colourless powder (4.83 g, 73.7%). TLC R_f 0.62 (4:1, EtOAc/MeOH); m.pt. 210.0–210.5 °C, m.pt. [33] 209–211 °C; ^{1}H NMR (DMSO-d_6) δ: 2.34 (3H, s, CH_3), 8.11 (1H, s, C2–H), 12.98 (1H, s, N3–H); ^{13}C NMR (DMSO-d_6) δ: 21.7 (CH_3), 119.8 (C-5), 146.7 (C-2), 157.1 (C-6), 160.3 (C-4); MS: (ES+) 145 (^{35}Cl M + H, 45%), 147 (^{37}Cl M + H, 12%), (ES−) 143 (^{35}Cl M + H, 50%). Elemental analysis: $C_5H_5ClN_2O$, calculated (%): C 41.54, H 3.49, N 19.38, Cl 24.52. Found (%): C 41.24, H 3.20, N 19.17, Cl 24.22.

4.2.11. 5-Chloro-6-(chloromethyl)-3H-pyrimidin-4-one (**36**)

A mixture of 5-chloro-6-methyl-3*H*-pyrimidin-4-one (4.00 g, 27.7 mmol, 1 eq), NCS (3.70 g, 27.7 mmol, 1 eq) and benzoyl peroxide (0.67 g, 2.77 mmol, 0.1 eq) in CCl_4 (200 ml) was heated at 80 °C for 96 h. The mixture was cooled to room temperature, the insoluble material was removed by filtration and the solvent was distilled off under reduced pressure. The residue was purified by column chromatography (DCM). The required fractions were pooled and evaporated giving the title compound **36** as a cream powder (0.51 g, 10.2%). TLC R_f 0.44 (4:1, EtOAc/MeOH); m.pt. 267–269.5 °C; ^{1}H NMR (DMSO-d_6) δ: 4.15 (2H, s, $-CH_2-$), 8.05 (1H, s, C2–H), 12.80 (1H, s, N3–H); ^{13}C NMR (DMSO-d_6) δ: 43.3 (CH_2), 120.3 (C-5), 147.3 (C-2), 156.3 (C-6), 160.5 (C-4).

4.2.12. 5-Chloro-6-[1-(2-iminopyrrolidinyl)methyl]-3H-pyrimidin-4-one hydrochloride (**18**)

A mixture of 5-chloro-6-(chloromethyl)-3*H*-pyrimidin-4-one (0.40 g, 2.24 mmol, 1 eq), 2-iminopyrrolidine hydrochloride (**37**) [45] (0.81 g, 6.70 mmol, 3 eq) and sodium ethoxide (0.46 g, 6.70 mmol, 3 eq) was stirred in anhydrous DMF (5.0 ml) under a N_2 atmosphere for 48 h at room temperature. The reaction mixture was filtered, the solid was added to water (3.5 ml) and neutralized with AcOH. The insoluble material was filtered, dissolved in 0.1 M HCl (15 ml), decolourized with activated charcoal, filtered through Celite and the filtrate was evaporated to dryness *in vacuo*. The solid was washed with a minimum volume of ethanol, filtered and dried to give the title compound **18** as a colourless powder (0.22 g, 38.1%). TLC R_f 0.18 (4:1, EtOAc/MeOH); m.pt. 286.5–287 °C; ^{1}H NMR (DMSO-d_6) δ: 2.04 (2H, quint, $^3J_{HH}$ = 7.5 Hz, $-CH_2-CH_2-CH_2-$), 2.87 (2H, t, $^3J_{HH}$ = 7.9 Hz, $-CH_2-C{=}NH_2^+$), 3.59 (2H, t, $^3J_{HH}$ = 7.3 Hz, $-CH_2-NH-$), 4.22 (2H, s, $-CH_2-$), 7.90 (1H, s, C2–H), 9.80 (1H, s, N^+H-H), 9.88 (1H, s, N^+H-H), 11.77 (1H, s, N3–H); ^{13}C NMR (DMSO-d_6) δ: 18.6 (C-4′), 31.5 (C-3′), 44.6 (C-5′), 52.3 ($-CH_2-$), 106.3 (C-5), 144.8 (C-6), 150.2 (C-2), 159.8 (C-4), 170.3 (C-2′); MS: (ES+) 228 (^{35}Cl M$^+$, 50%), 230 (^{37}Cl M$^+$, 16%). Elemental analysis: $C_9H_{12}Cl_2N_4O$, calculated (%): C 41.08, H 4.60, N 21.29. Found (%): C 40.81, H 4.31, N 21.02.

4.3. TP enzymology

The inhibition of recombinant *E. coli* TP and recombinant human TP, to determine the IC_{50} values of the compounds synthesized, was determined using a continuous spectrophotometric assay, adapted for a Molecular Devices Spectramax UV–visible spectrophotometer with a 96-well microplate reader, at a kinetic wavelength of 355 nm, at 25 °C. TP can convert 5-nitro-2′-deoxyuridine to 5-nitrouracil, this conversion was accompanied by a considerable change of absorption, at 355 nm, which was continuously monitored as a function of time [35]. The synthetic substrate 5-nitro-2′-deoxyuridine displays a higher extinction coefficient (ε_{max} 13,300 M^{-1} cm^{-1} at 322 nm) at a longer wavelength than thymidine (ε_{max} 9300 M^{-1} cm^{-1} at 266 nm), which provides additional sensitivity for assays. The nitro group decreases the value of k_{cat} of 5-nitro-2′-deoxyuridine (k_{cat} 20 s^{-1}; K_m 0.23 mM) by 88-fold compared to the methyl group of thymidine (k_{cat} 1770 s^{-1}; K_m 0.24 mM), but has little effect on the K_m value, with recombinant *E. coli* TP. Therefore the compromise in accepting the spectral convenience of the 5-nitro-2′-deoxyuridine substrate is decreased sensitivity [34].

The reaction mixtures (0.2 ml) contained 0.13 mM of 5-nitro-2′-deoxyuridine as the substrate and 0.1 M potassium phosphate buffer (pH 7.4). The reaction was initiated by addition of TP (0.00883 U/0.2 ml). The initial inhibitor stocks were prepared as 2.0–8.0 mM solutions and 50 μl of the stock was used in the assay, giving a final assay volume of 200 μl. If 50% inhibition was exceeded with 50 μl of the inhibitor stock, at 0.5–2.0 mM final cuvette concentration, the initial stock was serially diluted in 10-fold increments until a suitable level of TP inhibition was achieved. If no significant inhibition was observed at 1.0 mM the compound was not considered an inhibitor of TP. In the calculation of the IC_{50} value at least five inhibitor concentrations were used spanning the experimental value. The initial velocity was plotted against inhibitor concentration and the IC_{50} value was determined as the concentration causing a 50% decrease in the initial velocity relative to the mean of at least two controls with no inhibitor present. The human TP assay was conducted similarly except that 0.33 mM of 5-nitro-2′-deoxyuridine (K_m 0.16 mM) was used as substrate [34].

4.4. XO enzymology

The evaluation of the kinetic constants (K_m and V_{max}) for the natural substrate and prodrug activation by XO, from buttermilk, was determined using a continuous spectrophotometric assay, using a Unicam UV 300 Spectrometer with 3.5 ml Helma quartz cuvettes (1 cm light path) at 25 °C [36]. The reaction mixtures (3.0 ml) contained 50 mM potassium phosphate buffer (pH 7.5), the substrates in five different concentrations (25–150 μM). The reaction was initiated by injection of XO (0.9 U/ml). In the XO assay the enzyme concentration remained fixed and limiting so that the observed activity was proportional to the amount of substrate present. The change in absorbance was continually monitored over a time period at a specific predetermined wavelength, corresponding to the formation of the corresponding TP inhibitor. The absorption maxima was measured at a selected wavelength for each compound, substrate and product, in 50 mM

potassium phosphate buffer (pH 7.5), and plotted against concentration, the slope giving the molar absorption coefficient of the given compound. The initial reaction rates were recalculated using the molar absorption coefficients at the relevant wavelength for the product formed.

In the case of xanthine, the reaction mixtures (3.0 ml) contained 50 mM potassium phosphate buffer (pH 7.5) and 0.15 mM xanthine solution (pH 7.5). The reaction was initiated by injection of XO (0.9 U/ml). The formation of uric acid was monitored at 292 nm over a period of time [47]. The change of absorbance was taken as a measure of the reaction and the enzyme velocity was defined in terms of the change of absorbance per unit time [48]. The linear part of the curve is proportional to the initial velocity, the enzyme concentration remained fixed and limiting, therefore the absorbance is directly proportional to the concentration of product formed or substrate consumed. A series of reactions were performed at varying xanthine concentrations (50–150 μM). The initial rate generally follows saturation kinetics with respect to the concentration of the substrate. The determination of the values K_m and V_{max} were made from rearrangements of the Michaelis–Menten equation [49]. The velocity was recalculated from change in absorbance per minute using the molar absorption coefficient to determine the velocity in terms of μM/min (calculated from the mean of three independent measurements). The plot of absorbance at 292 nm versus concentration of uric acid gave a molar extinction coefficient of 12,500 M^{-1} cm^{-1}, which was in agreement with the literature [36]. The absorption maxima of 6A5BU was measured over a concentration range at a wavelength of 270 nm giving a molar extinction coefficient of 13,600 M^{-1} cm^{-1}. The absorption maxima of 7-DX was measured over a concentration range at 278 nm giving a molar extinction coefficient of 14,700 M^{-1} cm^{-1}. The absorption maxima of TPI was measured over a concentration range at 302 nm giving a molar extinction coefficient of 11,200 M^{-1} cm^{-1}.

4.5. Molecular modelling with human TP

Computational modelling was performed using the modelling package SYBYL 6.8 (Tripos Ltd.). The crystallographic coordinates for the 2.1 Å structure of human TP bound to the potent inhibitor TPI (PDB code: 1UOU) were obtained from AstraZeneca [42]. The ligands (both TP inhibitors and XO prodrugs) were constructed using SYBYL 6.8, and the atoms assigned partial atomic charges according to the Gasteiger–Marsili scheme. Once constructed, the inhibitors were modelled into the active site of the human TP crystal structure, using the experimental bound geometry of the inhibitor TPI as a guide (in a particular orientation of the nucleobase moiety). A 6 Å radius subset encompassing the TP active site–ligand complex was then minimized to convergence of 0.001 kcal/mol using the Tripos force field [41].

Acknowledgements

We thank Professor K.T. Douglas and Dr. E. Chinje for helpful discussions. This work was funded in part by the MRC and The Great Socialist People's Libyan Arab Jamahiriya (The Secretariat of Higher Education, Professor Akeel Hussain Akeel).

References

[1] S. Takao, S.I. Akiyama, A. Nakajo, H. Yoh, M. Kitazono, S. Natsugoe, K. Miyadera, M. Fukushima, Y. Yamada, T. Aikou, Cancer Res. 60 (2000) 5345–5348.
[2] M. Kitazono, Y. Takebayashi, K. Ishitsuka, S. Takao, A. Tani, T. Furukawa, K. Miyadera, Y. Yamada, T. Aikou, S. Akiyama, Biochem. Biophys. Res. Commun. 253 (1998) 797–803.
[3] K. Miyadera, T. Sumizawa, M. Haraguchi, H. Yoshida, W. Konstanty, Y. Yamada, S. Akiyama, Cancer Res. 55 (1995) 1687–1690.
[4] M. Haraguchi, K. Miyadera, K. Uemura, T. Sumizawa, T. Furukawa, K. Yamada, S.I. Akiyama, Nature 368 (1994) 198.
[5] M. Fukushima, N. Suzuki, T. Emura, S. Yano, H. Kazuno, Y. Tada, Y. Yamada, T. Asao, Biochem. Pharmacol. 59 (2000) 1227–1236.
[6] B.C. Pan, Z.H. Chen, M.Y. Wang Chu, S.H. Chu, Nucleosides Nucleotides 17 (1998) 2367–2382.
[7] C. Desgranges, G. Razaka, M. Rabaud, P. Picard, F. Dupuch, H. Bricaud, Biochem. Pharmacol. 31 (1982) 2755–2759.
[8] P. Langen, G. Etzold, D. Barwolff, B. Preussel, Biochem. Pharmacol. 16 (1967) 1833–1837.
[9] J. Balzarini, A.E. Gamboa, R. Esnouf, S. Liekens, J. Neyts, E. De Clercq, M.J. Camarasa, M.J. Perez-Perez, FEBS Lett. 438 (1998) 91–95.
[10] S. Yano, Y. Tada, H. Kazuno, T. Sato, J. Yamashita, N. Suzuki, T. Emura, M. Fukushima, T. Asao, PCT Int. Appl. (1996) 108.
[11] N. Suzuki, M. Fukushima, T. Asao, Y. Yamada, S. Akiyama, Proc. Am. Assoc. Cancer Res. 38 (1997) 101.
[12] P. Reigan, P.N. Edwards, A. Gbaj, C. Cole, S.T. Barry, K.M. Page, S.E. Ashton, R.W.A. Luke, K.T. Douglas, I.J. Stratford, M. Jaffar, R.A. Bryce, S. Freeman, J. Med. Chem. 48 (2005) 392–402.
[13] C. Cole, D.S. Marks, M. Jaffar, I.J. Stratford, K.T. Douglas, S. Freeman, Anticancer Drug Des. 14 (1999) 411–420.
[14] L.S. Terada, D. Piermattei, G.N. Shibao, J.L. McManaman, R.M. Wright, Arch. Biochem. Biophys. 348 (1997) 163–168.
[15] W.B. Poss, T.P. Hueckstedt, P.C. Panus, B.A. Freeman, J.R. Hoidal, Am. J. Physiol. 270 (1996) L941–L946.
[16] N.M. Hasan, R.B. Cundall, G.E. Adams, Free Radic. Biol. Med. 11 (1991) 179–185.
[17] H. Biri, H.S. Ozturk, M. Kacmaz, K. Karaca, H. Tokucoglu, I. Durak, Cancer Invest. 17 (1999) 314–319.
[18] H.S. Ozturk, M. Karaayvaz, M. Kacmaz, M. Kavutcu, H. Akgul, I. Durak, Cancer Biochem. Biophys. 16 (1998) 157–168.
[19] E. Kökoglu, A. Belce, E. Ozyurt, Z. Tepeler, Cancer Lett. 50 (1990) 179–181.
[20] M. Maliepaard, A. Wolfs, S.E. Groot, N.J. de Mol, L.H. Janssen, Br. J. Cancer 71 (1995) 836–839.
[21] C.A. Pritsos, D.L. Gustafson, Oncol. Res. 6 (1994) 477–481.
[22] E.D. Clarke, K.H. Goulding, P. Wardman, Biochem. Pharmacol. 31 (1982) 3237–3242.
[23] K. Shanmuganathan, T. Koudriakova, S. Nampalli, J. Du, J.M. Gallo, R.F. Schinazi, C.K. Chu, J. Med. Chem. 37 (1994) 821–827.
[24] T.A. Krenitsky, W.W. Hall, P. de Miranda, L.M. Beauchamp, H.J. Schaeffer, P.D. Whiteman, Proc. Natl. Acad. Sci. U.S.A. 81 (1984) 3209–3213.
[25] P. Reigan, A. Gbaj, E. Chinje, I.J. Stratford, K.T. Douglas, S. Freeman, Bioorg. Med. Chem. Lett. 14 (2004) 5247–5250.
[26] D.J. Brown, J.S. Harper, J. Chem. Soc. 1 (1961) 1298–1303.
[27] T. Sakamoto, C. Satoh, K. Yoshinori, H. Yamanaka, Chem. Pharm. Bull. 41 (1993) 81–86.
[28] D.E. Ayer, G.L. Bundy, E.J. Jacobsen, PCT Int. Appl. (1993) 120.
[29] D.G. Bartholomew, P. Dea, R.K. Robins, G.R. Revankar, J. Org. Chem. 40 (1975) 3708–3713.

[30] F. Seela, R. Richter, Chem. Ber. 111 (1978) 2925–2930.
[31] J. Davoll, J. Chem. Soc. (1960) 131–138.
[32] H.R. Snyder, H.M. Foster, G.A. Nussberger, J. Am. Chem. Soc. 76 (1954) 2441–2443.
[33] T. Nishiwaki, Tetrahedron 22 (1966) 2401–2408.
[34] A. Gbaj, P. Reigan, P.N. Edwards, S. Freeman, M. Jaffar, K.T. Douglas, J. Enzyme Inhib. Med. Chem. 21 (2006) 69–73.
[35] Y. Wataya, D.W. Santi, Anal. Biochem. 112 (1981) 96–98.
[36] H. Rosemeyer, F. Seela, Eur. J. Biochem. 134 (1983) 513–515.
[37] R.S. Klein, M. Lenzi, T.H. Lim, K.A. Hotchkiss, P. Wilson, E.L. Schwartz, Biochem. Pharmacol. 62 (2001) 1257–1263.
[38] J. Balzarini, B. Degreve, A. Esteban-Gamboa, R. Esnouf, E. De Clercq, Y. Engelborghs, M.J. Camarasa, M.J. Perez-Perez, FEBS Lett. 483 (2000) 181–185.
[39] P.E. Murray, V.A. McNally, S.D. Lockyer, K.J. Williams, I.J. Stratford, M. Jaffar, S. Freeman, Bioorg. Med. Chem. 10 (2002) 525–530.
[40] T.A. Krenitsky, S.M. Neil, G.B. Elion, G.H. Hitchings, Arch. Biochem. Biophys. 150 (1972) 585–599.
[41] M. Clark, R.D. Cramer, N. van Opdenbosch, J. Comput. Chem. 10 (1989) 982–1012.
[42] R.A. Norman, S.T. Barry, M. Bate, J. Breed, J.G. Colls, R.J. Ernill, R.W. Luke, C.A. Minshul, M.S. McAlister, E.J. McCall, H.H. McMiken, D.S. Paterson, D. Timms, J.A. Tucker, R.A. Pauptit, Structure 12 (2004) 75–84.
[43] E.F. Schroeder, US Patent, Searle 038 US 2731465. Chem. Abstr. 51 (1957) 1257.
[44] R.A. West, H.W. Barrett, J. Am. Chem. Soc. 76 (1953) 3146–3148.
[45] E.J. Moriconi, A.A. Cevasco, J. Org. Chem. 33 (1968) 2109–2111.
[46] R.H. Wollenberg, K.F. Albizati, R. Peries, J. Am. Chem. Soc. 99 (1977) 7365–7367.
[47] H. Kalckar, J. Biol. Chem. 167 (1947) 429–443.
[48] M. Dixon, E.C. Webb (Eds.), Enzymes, Longman, London, 1979.
[49] H. Lineweaver, D. Burk, J. Am. Chem. Soc. 56 (1934) 658–666.